Mem. S.A.It. Vol. 90, 347

Memorie della

Multiplicity statistics and properties across the HR diagram

M. Moe

University of Arizona, Steward Observatory, 933 N. Cherry Ave., Tucson, AZ 85721, USA
e-mail: moem@email.arizona.edu

Abstract. It is well established that the main-sequence binary fraction increases with primary mass, but we have only recently explored in detail other important parameters such as age, metallicity, and environment. In this proceeding, I overview recent observations that demonstrate the close binary fraction ($a \lesssim 10$ AU) of solar-type stars decreases with metallicity but is relatively constant with respect to age or environmental density, while the wide binary fraction ($a \gtrsim 1{,}000$ AU) is metallicity invariant but decreases dramatically during the pre-main-sequence phase. Wider binaries are intrinsically weighted toward smaller mass ratios, a trend that is especially evident for companions to massive OB primaries. I also discuss the properties of white dwarfs in binaries and the statistics of triples and higher-ordered multiples. I explain the various correlations with respect to mass and orbital separation in the context of protobinary fragmentation, accretion, and migration.

1. Introduction

The bias-corrected binary and multiple star statistics as a function of spectral type were extensively reviewed by Duchêne & Kraus (2013) and Moe & Di Stefano (2017). In the following, I discuss these statistical distributions in the context of binary star formation: disk fragmentation, accretion, and inward migration produce close binaries with $a < 10$ AU, turbulent fragmentation of molecular cores form wide binaries with $a > 1{,}000$ AU, and both modes contribute to the census of binaries with intermediate separations (Bate et al. 1995; Kroupa 1995; Bate et al. 2002; Kratter & Matzner 2006; Clarke 2009; Offner et al. 2010; Kratter & Lodato 2016; Moe et al. 2019). The main-sequence (MS) binary fraction $F_{\rm bin}$ and multiplicity frequency $f_{\rm mult}$ monotonically increase with primary mass (Section 2). Late-M and solar-type field binaries follow log-normal separation distributions peaking at $a \approx 10$ AU and ≈ 50 AU, respectively, and inner companions to more massive OB primaries become increasingly skewed toward shorter separations $a < 1$ AU (Section 3). The distribution of mass ratios $q = M_{\rm comp}/M_1$ of close binaries is roughly uniform with a small excess fraction of twins with $q > 0.95$, especially close solar-type binaries, while wide binaries are weighted toward small mass ratios, especially wide tertiary companions to OB primaries (Section 4). Most compact solar-type triples with $a_{\rm out} < 10$ AU are in nearly coplanar configurations, while wide tertiary companions beyond $a_{\rm out} > 1{,}000$ AU exhibit random orientations with respect to the inner binaries (Section 5). Although the wide binary fraction, close binary fraction of OB stars, and initial mass function (IMF) are metallicity invariant, the close binary fraction of solar-type stars is strongly anti-correlated with metallicity (Section 6). The wide binary fraction of late-type binaries decreases dramatically during the pre-MS phase due to dynamical processing in their birth clusters, while close binaries vary only marginally with respect to age or environment (Section 7).

2. Binary fraction and multiplicity frequency

In this section, I summarise two statistical quantities: the binary star fraction $F_{\rm bin}(M_1)$, which is the fraction of MS primaries with at least one *stellar MS companion* with $q > 0.1$, and the multiplicity frequency $f_{\rm mult}(M_1)$, which is the average frequency of stellar MS companions with $q > 0.1$ per primary. In Fig. 1, I show both $F_{\rm bin}(M_1)$ and $f_{\rm mult}(M_1)$ for MS primaries (black data points), and the solar-type values during the Class 0/I pre-MS phase (red data points). These statistics exclude sub-stellar brown dwarf (BD) companions as well as compact remnant companions such as white dwarfs (WDs), neutron stars (NSs), or black holes (BHs).

After utilising several observational techniques and correcting for various selection effects, Duquennoy & Mayor (1991) measured the binary star fraction of field solar-type primaries to be $F_{\rm bin} = 0.57 \pm 0.05$. Raghavan et al. (2010) estimated the binary star fraction and multiplicity frequency of solar-type stars within <25 pc to be $F_{\rm bin} = 0.46 \pm 0.02$ and $f_{\rm mult} = 0.59 \pm 0.05$, respectively. The observed binary fraction in the Tokovinin (2014) 67-pc sample of FG-dwarfs is $F_{\rm bin} = 0.42$, which is a lower limit due to incompleteness of late-M companions across intermediate separations. The difference $\Delta F_{\rm bin} = 0.11$ between Duquennoy & Mayor (1991) and Raghavan et al. (2010) is mainly because the former added undetected WD companions during their corrections for incompleteness. Moe & Di Stefano (2017) found $11\% \pm 4\%$ of solar-type MS stars in the field have WD companions ($\approx 20\%$ of all companions; see also Murphy et al. 2018), and so the inclusion versus exclusion of WD companions leads to the discrepancy between the observed field and zero-age MS solar-type binary star fractions.

The binary fraction of field M-dwarfs is measurably smaller (Fischer & Marcy 1992; Basri & Reiners 2006; Joergens 2006; Law et al. 2008; Bergfors et al. 2010; Janson et al. 2012; Dieterich et al. 2012; Ward-Duong et al. 2015; Winters et al. 2019). For early-M primaries ($M_1 = 0.3$ - 0.6M$_\odot$), the binary fraction is $F_{\rm bin} \approx 0.35$ - 0.40 and the multiplicity frequency is $f_{\rm mult} \approx 0.45$ - 0.50. For late M-dwarfs ($M_1 = 0.08$ - 0.3M$_\odot$), the binary star fraction is only $F_{\rm bin} \approx 0.20$ - 0.25, and the triple star fraction is negligible, i.e., $f_{\rm mult} \approx F_{\rm bin}$.

The binary star fraction is $F_{\rm bin} = 0.69 \pm 0.07$ for A-type primaries (De Rosa et al. 2014), $F_{\rm bin} > 0.8$ for B-type primaries (Abt et al. 1990; Kouwenhoven et al. 2007; Kobulnicky & Fryer 2007), and $F_{\rm bin} > 0.85$ for O-type primaries (Mason et al. 1998; Sana et al. 2014; Moe & Di Stefano 2017). After correcting for selection effects, the multiplicity frequency is $f_{\rm mult} = 1.35 \pm 0.25$ for B-type primaries (Rizzuto et al. 2013), $f_{\rm mult} = 1.9 \pm 0.3$ for early-B primaries (Abt et al. 1990), and $f_{\rm mult} = 2.2 \pm 0.3$ for O-type primaries (Sana et al. 2012). The multiplicity frequency of OB primaries is close to $\approx$2, implying the majority of massive stars are in triples and higher-ordered multiples. While only $\approx$13% of solar-type MS primaries are in triples and higher-ordered multiples (Raghavan et al. 2010; Tokovinin 2014), $\approx$60 - 80% of OB stars are in triples (Moe & Di Stefano 2017).

3. Period distribution

The binary period distributions provide insight into the fragmentation and migration processes of binary stars, and are used to determine the fraction of binaries that are close enough to interact. In Fig. 2, I show the frequency $f_{\rm logP}$ of MS companions per decade of orbital period as a function of M_1 and $\log P$ (adaptation from Moe & Di Stefano 2017). The companion frequency $f_{\rm logP}$ describes the period distribution of all companions, including inner binaries and outer tertiaries. Nearly all companions with $P < 100$ days are members of inner

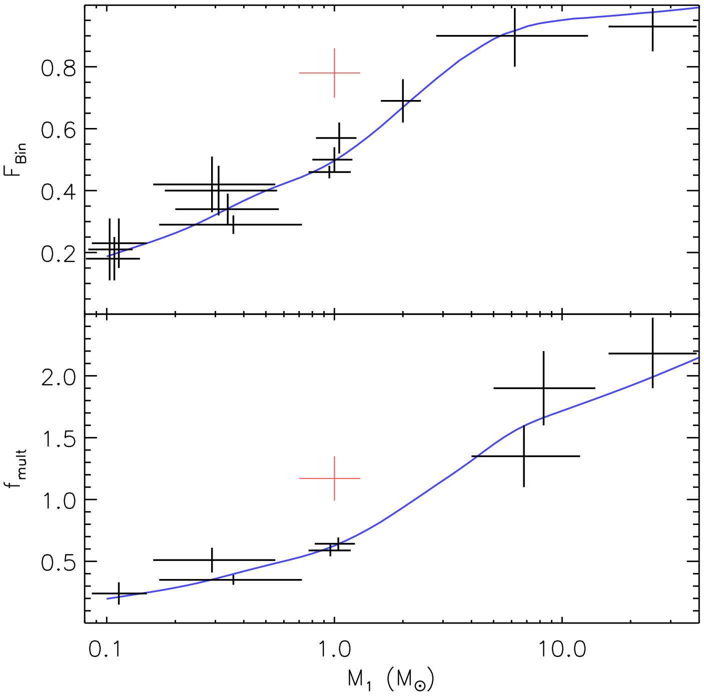

Fig. 1. The binary star fraction (top) and multiplicity frequency (bottom) of MS stars as a function of primary mass. The blue curves derive from integrating the period distributions of inner binaries (top) and all companions (bottom) based on the analytic fit presented in Moe & Di Stefano (2017, see also Section 3). The binary fraction and multiplicity frequency of solar-type pre-MS stars (thin red) are larger than their MS counterparts in the field, but are still less than the observed values for OB MS stars.

binaries (Tokovinin 2014; Sana et al. 2014). Meanwhile, at longer periods $\log P\,(\text{days}) > 7$, more than half of companions to solar-type MS primaries (Raghavan et al. 2010; Tokovinin 2014) and nearly all companions to OB primaries (Sana et al. 2014; Moe & Di Stefano 2017) are outer tertiaries in hierarchical triples. The resulting period distributions of only those companions that are members of inner binaries are shown as the thin lines in Fig. 2.

Duquennoy & Mayor (1991), Raghavan et al. (2010), Tokovinin (2014) all demonstrated companions to field solar-type MS primaries follow a log-normal period distribution with a peak at $\log P\,(\text{days}) = 4.8$ - 5.0 ($a \approx 50$ AU), dispersion of $\sigma_{\log P} = 2.3$, and normalisation such that $f_{\rm mult} = \int f_{\log P}\, {\rm d}\log P \approx 0.6$ (dotted line in Fig. 2). The separations of early-M binaries also follow a log-normal distribution, but with a slightly smaller mean separation $a \approx 30$ AU (Fischer & Marcy 1992; Janson et al. 2012; Ward-Duong et al. 2015; Winters et al. 2019). The separation distribution of binaries with late-M primaries with $M_1 = 0.08$ - $0.15\,{\rm M}_\odot$ narrowly peaks near $a \approx 7$ AU, exhibiting a dearth of systems beyond $a \gtrsim 100$ AU (Bouy et al. 2003; Basri & Reiners 2006; Winters et al. 2019). The companion frequency $f_{\log P} \approx 0.05$ across intermediate separations $a \approx 1$ - 10 AU is nearly constant between $M_1 = 0.1\,{\rm M}_\odot$ and $M_1 = 1\,{\rm M}_\odot$ (Murphy et al. 2018). The smaller M-dwarf binary fraction is therefore largely due to the relative deficit of wide companions.

For B-type MS primaries, the close binary fraction inferred from eclipsing and spectro-

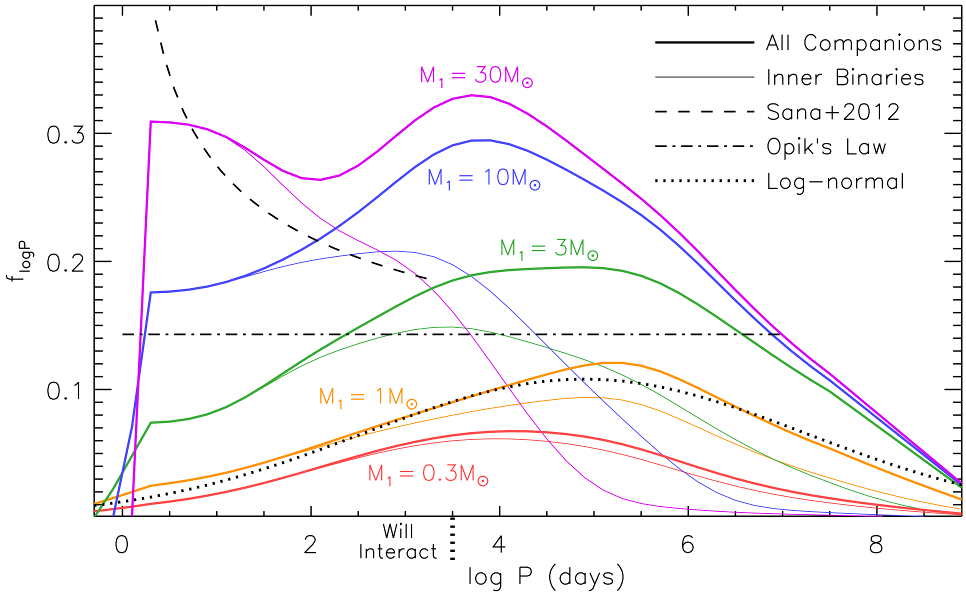

Fig. 2. Coloured according to primary mass M_1, analytic fit to the measured frequency f_{logP} of all companions (thick) and inner binaries (thin) per decade of orbital period (Moe & Di Stefano 2017). Integrating the thick and thin curves provide the multiplicity frequency $f_{\mathrm{mult}}(M_1)$ and binary star fraction $F_{\mathrm{bin}}(M_1)$, respectively. Field solar-type MS binaries follow a log-normal period distribution that peaks at log P (days) ≈ 4.9 (dotted; Duquennoy & Mayor 1991; Raghavan et al. 2010; Tokovinin 2014). Field M-dwarf binaries also follow a log-normal period distribution, but with a peak at slightly shorter periods (Winters et al. 2019, references therein). Inner binary companions to B-type MS primaries approximately obey Opik's law, i.e., a uniform distribution in log P (dash-dotted; Abt et al. 1990; Kouwenhoven et al. 2007; Kobulnicky & Fryer 2007). Inner binary companions to O-type MS primaries are skewed significantly toward very short periods (dashed; Sana et al. 2012). Close binaries with log P (days) $\lesssim$ 3.5 (left of thick dotted line) will eventually interact via Roche-lobe overflow.

scopic binaries (Levato et al. 1987; Abt et al. 1990; Moe & Di Stefano 2013) and the wide binary fraction measured with direct imaging and adaptive optics (Abt et al. 1990; Shatsky & Tokovinin 2002) are both larger than the values for solar-type MS primaries. The similarity in the measurements of $f_{\mathrm{logP}} \approx 0.15$ at both close and wide separations led Kouwenhoven et al. (2007) and Kobulnicky & Fryer (2007) to infer the period distribution of B-type MS binaries was consistent with Opik's law, i.e., a uniform distribution with respect to log P (dash-dotted line in Fig. 2). However, recent observations have filled in the gap at intermediate periods log P (days) = 3 - 5, demonstrating early-type binaries actually peak with $f_{\mathrm{logP}} \approx 0.20$ - 0.25 at such intermediate separations (Rizzuto et al. 2013; Evans et al. 2015; Moe & Di Stefano 2017; Murphy et al. 2018).

The close binary fraction of O-type MS primaries is even larger (Sana et al. 2012; Chini et al. 2012; Kobulnicky et al. 2014). In particular, Sana et al. (2012) found 69% ± 9% of O-type MS primaries have companions with P < 1,500 days, and that the period distribution of inner companions is skewed toward very short periods P < 20 days (dashed line in Fig. 2). Other observational techniques, including lucky imaging (Peter et al. 2012), speckle interferometry (Mason et al. 2009), direct imaging with *HST* (Aldoretta et al. 2015), long baseline interferometry, sparse aperture masking, and adaptive optics (Sana et al. 2014) show the frequency of companions at intermediate and wide separations is larger for O-type MS primaries compared to intermediate-mass primaries. While inner companions to O-type primaries are weighted toward short periods as found in Sana et al. (2012), the distribution of all companions, including outer tertiaries and quaternaries, cover a much broader range of periods (see Fig. 2).

4. Mass-ratio distribution

Binary mass ratios are set by the processes of fragmentation and accretion, and so the measured mass-ratio distributions provide stringent tests for models of binary star formation. Most studies of binary stars fit a single power-law distribution $f_q \propto q^\gamma$ to the observed mass ratios (Shatsky & Tokovinin 2002; Sana et al. 2012; Peter et al. 2012; Duchêne & Kraus 2013; De Rosa et al. 2014). However, with large samples, it becomes evident that a single-parameter model cannot adequately fit the distribution across all mass ratios (Duquennoy & Mayor 1991; Halbwachs et al. 2003; Gullikson et al. 2016; Moe & Di Stefano 2017; Murphy et al. 2018; El-Badry et al. 2019). Moe & Di Stefano (2017) therefore adopted a three-parameter model: a power-law slope $\gamma_{\rm smallq}$ across small mass ratios q = 0.1 - 0.3, a power-law slope $\gamma_{\rm largeq}$ across large mass ratios q = 0.3 - 1.0, and an excess fraction $F_{\rm twin}$ of twins with mass ratios q > 0.95 (adaptation shown in Fig. 3). El-Badry et al. (2019) adopted a similar construction for lower-mass KM binaries, but with a break at q = 0.5 separating the two power-law components.

For solar-type binaries, there is a modest excess twin fraction $F_{\rm twin} \approx 0.20$ at short periods P < 100 days (Tokovinin 2000; Halbwachs et al. 2003). Solar-type (Raghavan et al. 2010) and A-type (De Rosa et al. 2014) binaries with intermediate separations $a \approx 1$ - 100 AU exhibit a smaller but statistically significant excess twin fraction $F_{\rm twin} \approx 0.05$ - 0.10. At wider separations a > 200 AU, the excess twin fraction was previously measured to be $F_{\rm twin}$ < 0.05, i.e., consistent with zero (Lépine & Bongiorno 2007; Raghavan et al. 2010). However, El-Badry et al. (2019) recently utilised *Gaia* common-proper-motion binaries to demonstrate solar-type and M-type primaries exhibit a small but statistically significant excess twin fraction of $F_{\rm twin} \approx 0.03$ and ≈ 0.06, respectively, across a = 400 - 4,000 AU. For more massive primaries $M_1 \gtrsim 2\,{\rm M}_\odot$, the excess twin fraction $F_{\rm twin} \lesssim 0.04$ is negligible beyond P > 20 days (Abt et al. 1990; Shatsky & Tokovinin 2002; Moe & Di Stefano 2015b; Gullikson et al. 2016; Murphy et al. 2018). Only at very short periods P < 20 days do early-type MS binaries exhibit a small excess twin fraction $F_{\rm twin} \approx 0.10$ (Pinsonneault & Stanek 2006; Moe & Di Stefano 2013; Moe & Di Stefano 2017).

Close companions to both solar-type and early-type primaries roughly follow a uniform mass-ratio distribution, i.e., $\gamma_{\rm largeq} \approx \gamma_{\rm smallq} \approx 0.0$ (Abt et al. 1990; Raghavan et al. 2010; Sana et al. 2012). The mass-ratio distribution of solar-type binaries with intermediate separations $a \approx 10$ AU broadly peaks at $q \approx 0.3$ as found in Duquennoy & Mayor (1991), i.e., $\gamma_{\rm largeq} \approx -0.5$ and $\gamma_{\rm smallq} \approx 0.5$. At wider separations a > 200 AU, the mass-ratio distribution of solar-type binaries becomes weighted toward smaller mass ratios q = 0.3 ($\gamma_{\rm largeq} \approx -1.0$) and flattens below q < 0.3 ($\gamma_{\rm smallq} \approx 0.0$), but is still top heavy compared to random pairings drawn from the IMF (Lépine & Bongiorno 2007; Moe & Di Stefano 2017; El-Badry et al. 2019).

For early-type binaries, the power-law components $\gamma_{\rm largeq}$ and $\gamma_{\rm smallq}$ also decrease with increasing separation, but much more dramatically (see Fig. 3). For A-type and late-B primaries, the fitted values are $\gamma_{\rm largeq} \approx -1.0$

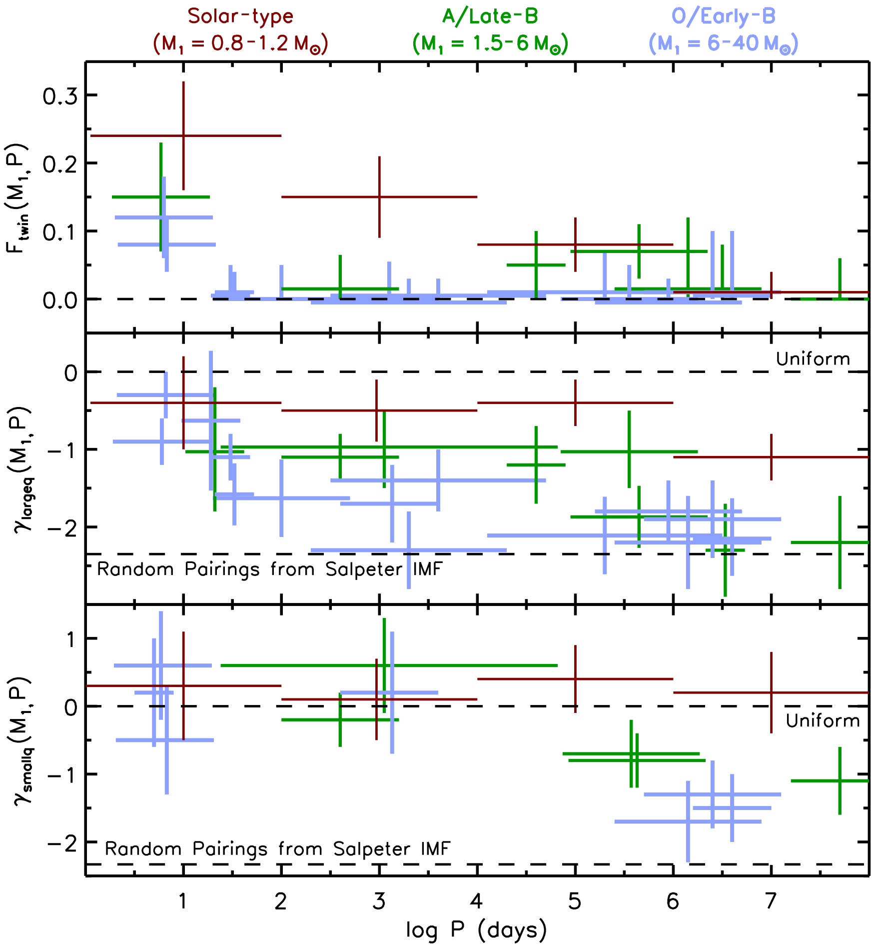

Fig. 3. The mass-ratio distribution as parameterised by the excess fraction F_{twin} of twins with $q > 0.95$ (top), power-law slope γ_{largeq} across large mass ratios q = 0.3 - 1.0 (middle), and power-law slope γ_{smallq} across small mass ratios q = 0.1 - 0.3 (bottom) as a function of period and coloured according to primary mass. Close binaries follow a uniform mass-ratio distribution ($\gamma_{\text{largeq}} = \gamma_{\text{smallq}} = 0.0$) with a small excess twin fraction F_{twin} = 0.1 - 0.2, while wider binaries become increasingly weighted toward smaller mass ratios, especially those with more massive primaries. Wide companions to early-type MS stars, mostly tertiaries, are significantly skewed toward extreme mass ratios, but their mass-ratio distribution is still mildly discrepant with random pairings drawn from a Salpeter IMF ($\gamma_{\text{largeq}} = \gamma_{\text{smallq}} = -2.35$).

and $\gamma_{\text{smallq}} \approx 0.0$ at intermediate separations $a \approx$ 1 - 100 AU (Shatsky & Tokovinin 2002; De Rosa et al. 2014; Gullikson et al. 2016; Murphy et al. 2018), which then decrease to $\gamma_{\text{largeq}} \approx -2.0$ and $\gamma_{\text{smallq}} \approx -1.0$ at very wide separations $a \gtrsim 500$ AU (De Rosa et al. 2014). Wide companions to more massive primaries become even further skewed toward smaller mass ratios. For early-B and O-type primaries, the power-law slopes are $\gamma_{\rm largeq} \approx -1.5$ and $\gamma_{\rm smallq} \approx 0.0$ across $a \approx 1$ - 10 AU (Abt et al. 1990; Rizzuto et al. 2013; Sana et al. 2014; Evans et al. 2015; Moe & Di Stefano 2015b) and $\gamma_{\rm largeq} \approx -2.0$ and $\gamma_{\rm smallq} \approx -1.5$ at wide separations $a \gtrsim 100$ AU (Abt et al. 1990; Peter et al. 2012; Sana et al. 2014). Even though wide companions to early-type MS stars are weighted significantly toward smaller mass ratios ($\gamma_{\rm largeq} \approx -2.0$), the mass-ratio distribution breaks below $q < 0.3$ ($\gamma_{\rm smallq} \approx -1.5$) and is therefore mildly discrepant with random pairings drawn from the IMF.

Close proto-binaries accrete from a circumbinary disk such that most of the infalling mass is directed via streams toward the lower-mass companion, driving inward migration and the mass ratio evolution toward unity (Bate et al. 1995; Kroupa 1995; Bate & Bonnell 1997; Clarke 2009; Young & Clarke 2015). This explains why close binaries exhibit a uniform mass-ratio distribution and an excess twin fraction. El-Badry et al. (2019) argued the few twins with a = 400 - 4,000 AU originally formed within the disk at closer separations, but then were subsequently widened due to N-body interactions in their birth clusters. Meanwhile, wide binaries that derive from core fragmentation are weighted toward small mass ratios with no excess of twins (Moe & Di Stefano 2017). The pre-MS mass-ratio distribution of very wide binaries ($a \sim 10{,}000$ AU) may have been initially consistent with random pairings drawn from the IMF, but the low-mass companions with lower binding energies have since been preferentially disrupted due to dynamical processing (Kroupa 1995).

Although it is difficult to detect companions with $q < 0.1$, a bias-corrected census of extreme mass-ratio binaries is beginning to emerge. Close solar-type binaries with $a \lesssim 1$ AU exhibit a dearth of q = 0.02 - 0.08 companions commonly known as the BD desert (Grether & Lineweaver 2006). At wider separations $a > 10$ AU, BD companions with $q < 0.1$ are as abundant as late-M companions with q = 0.1 - 0.2 (Kraus et al. 2011; Raghavan et al. 2010; Wagner et al. 2019). For binaries with A/F primaries and intermediate periods $P \approx 100$ - 1,000 days, there is a deficit of extreme mass-ratio binaries $q < 0.1$ compared to systems with q = 0.1 - 0.2, but not a complete absence as observed for solar-type systems (Murphy et al. 2018). For more massive B-type MS primaries, the frequency of companions with q = 0.05 - 0.10 appears to be as plentiful as companions with q = 0.10 - 0.15, even at very short periods $P < 10$ days (Moe & Di Stefano 2015a).

M-dwarf binaries are weighted toward more equal masses (see Winters et al. 2019 for a review). For early M-dwarf binaries with intermediate separations $a \approx 10$ AU, the mass-ratio distribution is nearly uniform with a turnover in the sub-stellar BD regime (Fischer & Marcy 1992; Bergfors et al. 2010; Janson et al. 2012; Winters et al. 2019). As observed for more massive binaries, there may be an intrinsic trend whereby wider companions to M-dwarfs systematically favour smaller mass ratios (Duchêne & Kraus 2013). For binaries with late M-dwarf primaries and intermediate separations $a \approx 1$ - 10 AU, the mass-ratio distribution is weighted significantly toward $q \gtrsim 0.7$. (Bouy et al. 2003; Joergens 2006; Basri & Reiners 2006; Bergfors et al. 2010; Dieterich et al. 2012; Duchêne & Kraus 2013; Winters et al. 2019). The mass-ratio distribution of late M-dwarf binaries can be modelled by either a large excess twin fraction $F_{\rm twin} \approx 0.4$ and/or a power-law slope $\gamma_{\rm largeq} \approx 2$ - 4 that is significantly skewed toward large mass ratios. As emphasised in Dieterich et al. (2012) and Duchêne & Kraus (2013), the dearth of BD companions to M-type primaries is not a selection bias but instead intrinsic to the population of M-dwarf binaries, similar to the BD desert observed for solar-type primaries.

5. Triples

The hierarchies of solar-type triples span the full parameter space f($a_{\rm in}$,$a_{\rm out}$) provided they are dynamically stable according to the criterion $a_{\rm out} \gtrsim 3a_{\rm in}$ (Tokovinin 2014). Compact solar-type triples with $a_{\rm out} < 10$ AU are in nearly co-planar configurations, i.e., $\approx$90% with mutual inclinations $i < 40°$ (Borkovits et al. 2016). Compact triples tend to be co-planar because both components derived from disk fragmentation, as in the case example resolved by ALMA (Tobin et al. 2016a). Meanwhile, Tokovinin (2017) showed that slightly wider solar-type triples with $a_{\rm out} \approx 50$ AU exhibit a broader distribution of mutual inclinations, but still with ≈90% in prograde configurations satisfying $i < 90°$. He also showed that only tertiaries with $a_{\rm out} \gtrsim 1{,}000$ AU, likely those that formed via core fragmentation, have equal proportions of prograde and retrograde orbits with respect to the inner binaries, suggestive of random orientations. There is a slight indication that the degree of triple-star misalignment increases with primary mass (Tokovinin 2017), but larger samples are needed to fully quantify this trend and dependence on orbital separation.

Only ≈30% of solar-type binaries with $P_{\rm in} > 20$ days have tertiary companions, but ≈80% of very close binaries with $P_{\rm in} < 7$ days are in triples. The latter led Kiseleva et al. (1998), Fabrycky & Tremaine (2007), and Naoz & Fabrycky (2014) to conclude that a significant fraction of very close binaries derived from Kozai-Lidov oscillations in misaligned triples coupled with tidal friction. However, Moe & Kratter (2017) showed that only a minority of very close binaries could have migrated via this mechanism because (1) most compact triples have $i < 40°$ and therefore could not undergo Kozai-Lidov cycles, and (2) the associated migration timescales are generally too long (> 10 Myr) to explain the observed population of very close pre-MS binaries (see Section 7). Moe & Kratter (2017) instead concluded that most very close binaries derive from migration within massive dissipative disks, and these massive disks also tend to produce compact co-planar tertiaries.

6. Metallicity variations

The spectroscopic binary fraction of solar-type stars *appears* to be independent of metallicity (Latham et al. 2002; Carney et al. 2005). However, both Grether & Lineweaver (2007) and Raghavan et al. (2010) found that the bias-corrected binary fraction decreases with metallicity, albeit with marginal significance. Badenes et al. (2018) subsequently utilized multi-epoch high-resolution APOGEE spectra to demonstrate the radial velocity (RV) variability fraction of metal-poor stars is ≈2 - 3 times larger than metal-rich stars. Moe et al. (2019) reanalysed these various samples, and demonstrated that because the absorption lines of metal-poor stars are weaker, the uncertainties in their RVs are systematically larger, and so it is more difficult to detect their spectroscopic RV companions. The true bias-corrected close binary fraction is therefore strongly anti-correlated with metallicity (see Fig 4). Moe et al. (2019) also examined the occurrence rate of Kepler eclipsing binaries, and discovered the same anti-correlation with respect to metallicity as found in the spectroscopic binary samples. As shown in Fig. 4, the bias-corrected close binary fraction within $a <$ 10 AU decreases from ≈55% at [Fe/H] = −3.0 to ≈40% at [Fe/H] = −1.0, and then to ≈10% at [Fe/H] = +0.5.

Conversely, Moe et al. (2019) examined various imaging surveys of solar-type stars and concluded that the wide binary fraction ($a >$ 200 AU) is independent of metallicity. El-Badry & Rix (2019) analysed *Gaia* common-proper-motion binaries with spectroscopic metallicity measurements and confirmed that the wide binary fraction beyond $a >$ 200 AU does not vary by more than ≈10% across −1.0 < [Fe/H] < 0.5, but that a metallicity dependence emerges below $a <$ 200 AU. At intermediate separations of $a \approx 50$ AU, they showed that the binary fraction decreases by a factor of ≈3.0 from [Fe/H] = −1.0 to +0.5, nearly the factor of ≈4.0 observed below $a <$ 10 AU.

Finally, unlike solar-type stars, the close binary fraction of OB stars is independent of metallicity (Moe & Di Stefano 2013). I display the bias-corrected binary period distributions as a function of primary mass and metallicity in Fig. 5. Moe et al. (2019) concluded that turbulent fragmentation of optically thin cores was independent of metallicity,

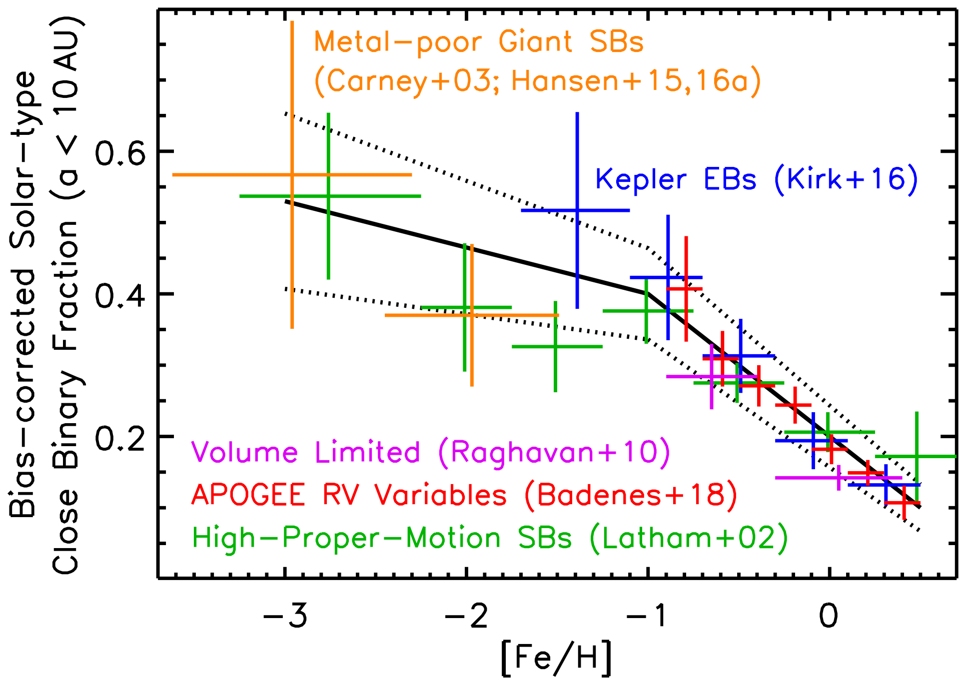

Fig. 4. The bias-corrected close binary fraction of solar-type stars taken from Moe et al. (2019). All five samples / methods yield consistent results, demonstrating the decrease in the close binary fraction with respect to metallicity is robust.

as shown in hydrodynamic simulations (Bate 2019), which is why the wide binary fraction and IMF are metallicity invariant. Meanwhile, optically thick disks become cooler and more prone to fragmentation with decreasing metallicity (Tanaka & Omukai 2014; Moe et al. 2019), which explains why the close binary fraction of solar-type stars is anti-correlated with metallicity. Even at solar metallicity, the disks of massive proto-stars are gravitationally unstable (Kratter & Matzner 2006; Tanaka & Omukai 2014; Kratter & Lodato 2016), and so the close binary fraction of OB stars is ≈100%. Decreasing the metallicity cannot therefore increase the propensity for disk fragmentation (binary formation is already saturated), and so their close binary fraction is metallicity invariant. The binary fraction within a < 200 AU of solar-type stars with [Fe/H] = −1.0 is also nearly saturated at ≈100%, possibly explaining the flattening in the close binary fraction below [Fe/H] $\lesssim$ −1.0 in Fig.4.

7. Pre-main-sequence

Most solar-type stars were initially born in binaries, but dynamical interactions disrupted the majority of wide companions on cluster-crossing timescales (Kroupa 1995). Far-IR and sub-mm observations of very young Class 0/I proto-stars reveal a large factor of ≈3 excess of wide companions beyond a > 500 AU relative to the field (Duchêne et al. 2007; Connelley et al. 2008; Tobin et al. 2016b). This excess quickly diminishes by the older Class II/III phase. Meanwhile, the close bi-

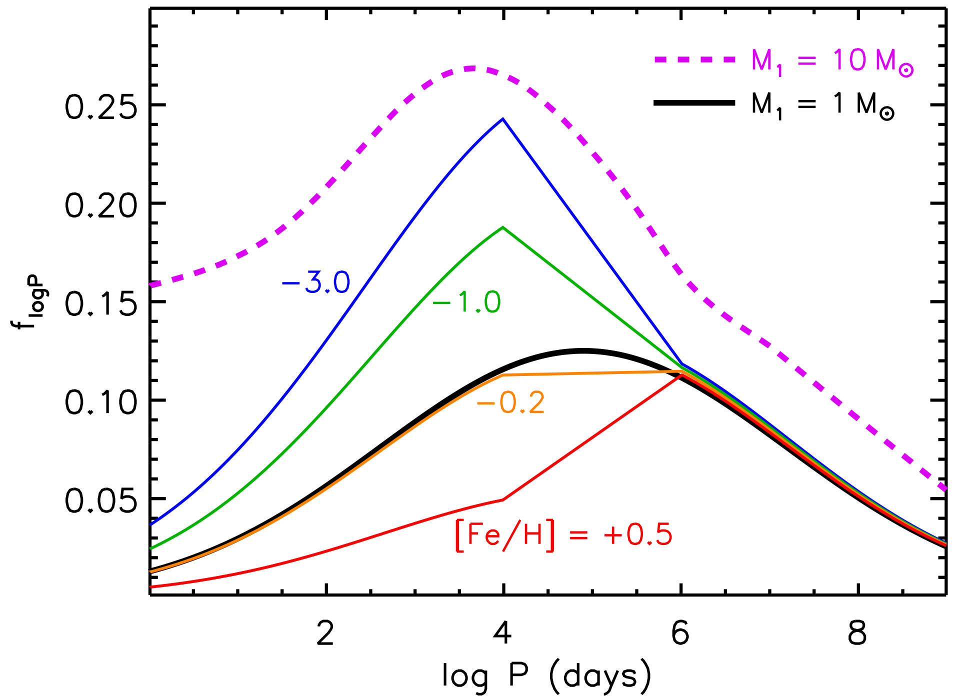

Fig. 5. The frequency of stellar companions per decade of orbital period as a function of primary mass and metallicity taken from Moe et al. (2019). I compare M_1 = 10M$_\odot$ primaries (thick dashed magenta; metallicity invariant), field solar-type binaries averaged across all metallicities (thick black), and the metallicity-dependent distributions for solar-type primaries (thin coloured).

nary fraction of T Tauri stars is consistent with the field (Mathieu 1994; Melo 2003; Kounkel et al. 2019). In particular, Kounkel et al. (2019) showed that the binary fraction and period distribution across P = 2 - 10,000 days (a = 0.05 - 10 AU) of class II/III T Tauri stars were nearly identical to the field properties, with at most a 30% deficit at the shortest of periods P < 5 days. The latter demonstrates that at most $\lesssim$30% of very close binaries migrate via Kozai-Lidov cycles in triples and tidal friction after the zero-age MS. Kounkel et al. (2019) also found the close binary fraction may change non-monotonically with density, but the observations were also consistent with no variation.

Interestingly, high-resolution and adaptive optics imaging of T Tauri stars in low-density environments reveal an excess of companions across intermediate separations $a \approx$ 10 - 100 AU (Ghez et al. 1993; Kraus et al. 2011, 2012). It was originally believed that all stars were initially born with an excess of companions beyond a > 10 AU relative to the field, but that dynamical interactions in dense environments like Orion reduced the binary fraction across such intermediate separations. This implied that most low-mass stars were born in such Orion-like environments in order for the simulated rate of dynamical disruptions across a = 10 - 100 AU to match the rate inferred from observations. However, Duchêne et al. (2018) showed that even young stars in Orion exhibit a large excess of companions across a = 10 - 100 AU. They concluded that most field stars must have been born in environments that significantly differed from all the nearby star forming environments we see today. The similarity in the period distribution and close binary fraction below a < 10 AU found between T Tauri stars and field stars and the excess of T Tauri binaries across a = 10 - 100 AU in Orion presents a significant challenge for theories and dynamical models of binary star formation.

8. Conclusions

Binary stars display a complicated parameter space in which the distributions of primary mass, period, mass ratio, eccentricity are all inter-related and depend on other parameters such as metallicity, age, and environment. The triple star fraction of massive stars, distributions of triple star hierarchies, and mutual inclinations of triples have only been recently measured. The various observational constraints suggest close binaries derived from disk fragmentation and migration while wide binaries formed via core fragmentation, but additional observations are needed to fill in the gaps and resolve apparent discrepancies between various data sets. The millions of eclipsing, spectroscopic, and astrometric binaries to be discovered by *Gaia* (Eyer et al. 2015) will help further constrain models of binary star formation. Most importantly, I showed some case examples where selection effects can bias our interpretations, e.g., inclusion (Duquennoy & Mayor 1991) versus exclusion (Raghavan et al. 2010) of WD companions when measuring the binary fraction of solar-type stars (Moe & Di Stefano 2017), or correcting for incompleteness as a function of metallicity (Moe et al. 2019). With future and larger samples of binary stars, it becomes even more imperative to account for the various selection effects.

Acknowledgements. I acknowledge financial support from NASA under grant ATP-170070.

References

Abt, H. A., Gomez, A. E., & Levy, S. G. 1990, ApJS, 74, 551
Aldoretta, E. J., Caballero-Nieves, S. M., Gies, D. R., et al. 2015, AJ, 149, 26
Badenes, C., Mazzola, C., Thompson, T. A., et al. 2018, ApJ, 854, 147
Basri, G. & Reiners, A. 2006, AJ, 132, 663
Bate, M. R. 2019, MNRAS, 484, 2341
Bate, M. R. & Bonnell, I. A. 1997, MNRAS, 285, 33
Bate, M. R., Bonnell, I. A., & Bromm, V. 2002, MNRAS, 336, 705
Bate, M. R., Bonnell, I. A., & Price, N. M. 1995, MNRAS, 277, 362
Bergfors, C., Brandner, W., Janson, M., & et al. 2010, A&A, 520, A54
Borkovits, T., Hajdu, T., Sztakovics, J., & et al. 2016, MNRAS, 455, 4136
Bouy, H., Brandner, W., Martín, E. L., & et al. 2003, AJ, 126, 1526
Carney, B. W., et al. 2005, AJ, 129, 1886
Chini, R., et al. 2012, MNRAS, 424, 1925
Clarke, C. J. 2009, MNRAS, 396, 1066
Connelley, M. S., Reipurth, B., & Tokunaga, A. T. 2008, AJ, 135, 2526
De Rosa, R. J., Patience, J., Wilson, P. A., & et al. 2014, MNRAS, 437, 1216
Dieterich, S. B., et al. 2012, AJ, 144, 64
Duchêne, G., Bontemps, S., Bouvier, J., & et al. 2007, A&A, 476, 229
Duchêne, G. & Kraus, A. 2013, ARA&A, 51, 269
Duchêne, G., et al. 2018, MNRAS, 478, 1825
Duquennoy, A. & Mayor, M. 1991, A&A, 248, 485
El-Badry, K. & Rix, H.-W. 2019, MNRAS, 482, L139
El-Badry, K., et al. 2019, arXiv e-prints, arXiv:1906.10128
Evans, N. R., Berdnikov, L., Lauer, J., & et al. 2015, AJ, 150, 13
Eyer, L., Rimoldini, L., Holl, B., & et al. 2015, in Living Together: Planets, Host Stars and Binaries, ed. S. M. Rucinski, G. Torres, & M. Zejda (ASP, San Francisco), ASP Conf. Ser., 496, 121
Fabrycky, D. & Tremaine, S. 2007, ApJ, 669, 1298
Fischer, D. A. & Marcy, G. W. 1992, ApJ, 396, 178
Ghez, A. M., Neugebauer, G., & Matthews, K. 1993, AJ, 106, 2005

Grether, D. & Lineweaver, C. H. 2006, ApJ, 640, 1051
Grether, D. & Lineweaver, C. H. 2007, ApJ, 669, 1220
Gullikson, K., Kraus, A., & Dodson-Robinson, S. 2016, AJ, 152, 40
Halbwachs, J. L., et al. 2003, A&A, 397, 159
Janson, M., Hormuth, F., Bergfors, C., & et al. 2012, ApJ, 754, 44
Joergens, V. 2006, A&A, 446, 1165
Kiseleva, L. G., Eggleton, P. P., & Mikkola, S. 1998, MNRAS, 300, 292
Kobulnicky, H. A. & Fryer, C. L. 2007, ApJ, 670, 747
Kobulnicky, H. A., Kiminki, D. C., Lundquist, M. J., & et al. 2014, ApJS, 213, 34
Kounkel, M., Covey, K., Moe, M., et al. 2019, AJ, 157, 196
Kouwenhoven, M. B. N., et al. 2007, A&A, 474, 77
Kratter, K. & Lodato, G. 2016, ARA&A, 54, 271
Kratter, K. M. & Matzner, C. D. 2006, MNRAS, 373, 1563
Kraus, A. L., et al. 2012, ApJ, 745, 19
Kraus, A. L., et al. 2011, ApJ, 731, 8
Kroupa, P. 1995, MNRAS, 277, 1507
Latham, D. W., Stefanik, R. P., Torres, G., & et al. 2002, AJ, 124, 1144
Law, N. M., Hodgkin, S. T., & Mackay, C. D. 2008, MNRAS, 384, 150
Lépine, S. & Bongiorno, B. 2007, AJ, 133, 889
Levato, H., et al. 1987, ApJS, 64, 487
Mason, B. D., Gies, D. R., Hartkopf, W. I., et al. 1998, AJ, 115, 821
Mason, B. D., et al. 2009, AJ, 137, 3358
Mathieu, R. D. 1994, ARA&A, 32, 465
Melo, C. H. F. 2003, A&A, 410, 269
Moe, M. & Di Stefano, R. 2013, ApJ, 778, 95
Moe, M. & Di Stefano, R. 2015a, ApJ, 801, 113
Moe, M. & Di Stefano, R. 2015b, ApJ, 810, 61
Moe, M. & Di Stefano, R. 2017, ApJS, 230, 15
Moe, M. & Kratter, K. M. 2017, ArXiv e-prints, arXiv: 1706.09894
Moe, M., Kratter, K. M., & Badenes, C. 2019, ApJ, 875, 61
Murphy, S. J., Moe, M., Kurtz, D. W., & et al. 2018, MNRAS, 474, 4322
Naoz, S. & Fabrycky, D. C. 2014, ApJ, 793, 137
Offner, S. S. R., et al. 2010, ApJ, 725, 1485
Peter, D., et al. 2012, A&A, 538, A74
Pinsonneault, M. H. & Stanek, K. Z. 2006, ApJ, 639, L67
Raghavan, D., McAlister, H. A., Henry, T. J., & et al. 2010, ApJS, 190, 1
Rizzuto, A. C., Ireland, M. J., Robertson, J. G., & et al. 2013, MNRAS, 436, 1694
Sana, H., de Mink, S. E., de Koter, A., & et al. 2012, Science, 337, 444
Sana, H., Le Bouquin, J.-B., Lacour, S., & et al. 2014, ApJS, 215, 15
Shatsky, N. & Tokovinin, A. 2002, A&A, 382, 92
Tanaka, K. E. I. & Omukai, K. 2014, MNRAS, 439, 1884
Tobin, J. J., Kratter, K. M., Persson, M. V., et al. 2016a, Nature, 538, 483
Tobin, J. J., Looney, L. W., Li, Z.-Y., & et al. 2016b, ApJ, 818, 73
Tokovinin, A. 2014, AJ, 147, 87
Tokovinin, A. 2017, ApJ, 844, 103
Tokovinin, A. A. 2000, A&A, 360, 997
Wagner, K., Apai, D., & Kratter, K. M. 2019, ApJ, 877, 46
Ward-Duong, K., Patience, J., De Rosa, R. J., & et al. 2015, MNRAS, 449, 2618
Winters, J. G., Henry, T. J., Jao, W.-C., et al. 2019, AJ, 157, 216
Young, M. D. & Clarke, C. J. 2015, MNRAS, 452, 3085